Synthesis, Structure, and Properties of New Perovskite $PbVO_3$

Roman V. Shpanchenko,* Viktoria V. Chernaya, Alexander A. Tsirlin, Pavel S. Chizhov, Dmitry E. Sklovsky, and Evgeny V. Antipov

Department of Chemistry, Moscow State University, 119992 Moscow, Russia

Evgeny P. Khlybov

Institute for High-Pressure Physics, 142092 Troitsk, Russia

Vladimir Pomjakushin

Laboratory for Neutron Scattering, ETH Zurich & PSI Villigen, CH-5232 Villigen PSI, Switzerland

Anatoly M. Balagurov

Frank Laboratory of Neutron Physics, JINR, 141980 Dubna, Russia

Julia E. Medvedeva

Institute of Solid State Chemistry, 620249 Ekaterinburg, Russia

Enrique E. Kaul and Christoph Geibel

Max-Planck Institute CPfS, Nöthnitzer Street 40, 01187 Dresden, Germany

Received April 29, 2004. Revised Manuscript Received June 14, 2004

The new perovskite $PbVO_3$ was synthesized under high-temperature and high-pressure conditions. Its crystal structure (a = 3.80005(6) Å, c = 4.6703(1) Å, Z = 1, S.G. $P4mm$) contains isolated layers of corner-shared VO_5 pyramids, which are formed instead of octahedra due to a strong tetragonal distortion (c/a = 1.23). The lead atom is shifted out of the center of the unit cell toward one of two $[VO_2]$-layers due to the influence of the lone pair. This new perovskite exhibits a semiconductor-like $\rho(T)$ dependence down to 2 K. This behavior can be qualitatively explained by taking into account strong electron correlations in electronic structure calculations.

Introduction

The rising interest in highly correlated electron systems called for an intensive investigation of reduced vanadium oxides. The perovskite-like compounds AVO_3, where A is a three or divalent cation, are widely studied due to their simple structures, which allow a deep understanding of the relationship between structure and properties in these systems.

AVO_3 oxides were reported for most of the divalent elements as A-cation. For alkali-earth elements (except Mg) their structures are three-dimensional frameworks consisting of corner-shared VO_6 octahedra. Octahedra in these structures are regular or slightly distorted and no formation of a short vanadyl bond is observed. Thus, $SrVO_3$ is an ideal cubic perovskite[1,2] and $CaVO_3$ is an orthorhombically distorted perovskite ($GdFeO_3$-type)[1,3] while $BaVO_3$ forms trigonal 5H close-packing in a wide range of oxygen nonstoichiometry.[4] Stoichiometric $CaVO_3$ and $SrVO_3$ compounds exhibit metallic-like conductivity down to 2−4 K and Pauli paramagnetic behavior. These properties can be changed by variation of oxygen content.[2,5−7]

Until now no information is available on the existence of $PbVO_3$ despite Pb^{2+} cation crystal radius (1.63 Å) being very close to that for Sr^{2+} (1.58 Å). The synthesis of this compound looks very attractive, taking into account the influence of the lone pair of the Pb^{2+} cation, which can lead to a strong distortion of the perovskite lattice and thus to a decrease of the dimensionality of the structure. Below, we present the results of the

* To whom correspondence should be addressed. E-mail: shpanchenko@icr.chem.msu.ru.

(1) Chamberland, B. L.; Danielson, P. S. *J. Solid State Chem.* **1971**, *3*, 243.
(2) Lan, Y. C.; Chen, X. L.; He, M. *J. Alloys Compd.* **2003**, *354*, 95.
(3) Garcia-Jaca, J.; Mesa, J. L.; Insausti, M.; Larramendi, J. I. R.; Arriortua, M. I.; Rojo, T. *Mater. Res. Bull.* **1999**, *34*, 289.
(4) Liu, G.; Greedan, J. E. *J. Solid State Chem.* **1994**, *110*, 274.
(5) Inoue, H.; Morikawa, K.; Fukuchi, H.; Tsujii, T.; Iga, F.; Nishihara, Y. *Physica B* **1994**, *194−196*, 1067.
(6) Inoue, I. H.; Makino, H.; Hase, I.; Ishikawa, M.; Hussey, N. E.; Rozenberg, M. J. *Physica B* **1997**, *237−238*, 61.
(7) Ueda, Y. *J. Solid State Chem.* **1998**, *135*, 36.

10.1021/cm049310x CCC: $27.50 © 2004 American Chemical Society
Published on Web 07/28/2004

synthesis and investigation of the new perovskite $PbVO_3$.

Experimental Section

We have explored different ways to prepare the Pb,V-perovskite and succeeded only with the application of a high-pressure high-temperature technique. The latter provides a unique possibility to obtain new structures which cannot be synthesized at ambient pressure conditions. The perovskite structure possesses a high density and may be often stabilized by high pressure as it happens, for example, in the case of $CdVO_3$.[8]

$PbVO_3$ was synthesized in a "lens"-type apparatus.[9] Simple oxides PbO, VO_2, or a mixture (1:1) of V_2O_3 and V_2O_5 were taken as initial reagents. Annealing temperature, pressure, and time of reaction were varied in the ranges 650−1000 °C, 40−80 kbar, and 5−240 min, respectively. The most pure $PbVO_3$ samples were obtained in 40−60 kbar pressure range and at 700−750 °C. At a lower temperature mainly initial reagents were present in the reaction mixture. Annealings at higher temperature were accompanied by the red-ox reactions, leading to the formation of metallic lead and compounds with pentavalent vanadium.

X-ray powder diffraction (XPD) data were collected on a STADI-P diffractometer (Cu $K\alpha_1$-radiation, linear PSD, transmission mode). The RIETAN2000 program[10] was used for structure refinement.

To investigate the presence of magnetic ordering, a neutron powder diffraction (NPD) experiment was carried out on the DMC diffractometer at the Swiss Spallation Neutron Source (SINQ). The DMC diffractometer, being situated at a supermirror-coated guide for cold neutrons, is very effective in studying magnetic structures, in particular for the determination of weak magnetic intensities. The 0.3-cm^3 powder sample was placed in a cylindrical Al can. The Al can was used instead of a V one to minimize the incoherent background and hence to improve the accuracy of the magnetic moment determination. An oscillating radial collimator suppressed Bragg peaks from the sample environment. For the purpose of magnetic structure determination, long-statistics powder neutron diffraction profiles for $PbVO_3$ were collected in the range $7 \le 2\theta \le 87°$ (step 0.2°) over a 8-h period at two temperatures 1.5 and 120 K, using a neutron wavelength $\lambda = 2.567$ Å. Rietveld refinements of the powder neutron diffraction patterns were performed with the FULLPROF[11] suite of powder diffraction software, using its internal tables of neutron scattering lengths and magnetic form factors.

The bonding character in the structure was analyzed using the electron localization function (ELF).[12] ELF distribution was calculated with the TB-LMTO-ASA program package[13] after SCF calculation. For the basis the 6s and 6p orbitals of Pb, 4s, 4p, and 3d orbitals of V, and the 2s and 2p orbitals of O were used directly and the 5d orbitals of Pb by a downfolding technique. Barth-Hedin exchange-correlation potential was used in DFT calculation; the calculation was performed for 125 k-points in the irreducible Brillouin zone. ELF distribution was obtained using the intrinsic procedure of the program.

Resistivity measurements were carried out between 2 and 300 K on a pellet in commercial equipment (PPMS) using a standard four-point AC method; susceptibility measurements were carried out between 2 and 300 K in fields between 0.1 and 5 T in a commercial Squid magnetometer (PPMS).

Results

Crystal Structure of $PbVO_3$. The X-ray powder diffraction pattern of $PbVO_3$ was indexed in a tetragonal cell with lattice parameters $a = 3.79995(8)$ Å, $c = 4.6704(2)$ Å, and $Z = 1$. Attempts to synthesize $PbVO_{3\pm\delta}$ ($0 \le \delta \le 0.3$) with different oxygen content always resulted in polyphasic mixtures containing $PbVO_3$ as a main product and admixtures of three- or pentavalent vanadium oxides. Regardless of synthesis conditions and various admixtures present in the samples, the cell parameters of $PbVO_3$ were identical in all samples. This may indicate a narrow homogeneity range and the absence of a noticeable oxygen nonstoichiometry.

$PbVO_3$ completely decomposes, being heated in an evacuated quartz ampule at 300−400 °C. We failed to synthesize this compound using a solid state reaction at different ambient pressure conditions. Its formation was never observed after annealing either in evacuated or Ar-filled quartz ampules or in dynamic vacuum. In contrast, this oxide can readily be obtained under high pressure. Moreover, under pressure, $PbVO_3$ was often observed as an admixture even in cases when the bulk composition of the initial mixture strongly differed from the stoichiometric one.

XPD patterns of all prepared samples contained admixture peaks of different phases. The most pure sample used for structure refinement contained additionally $Pb_3(CO_3)_2(OH)_2$ and PbV_6O_{11}. No other reflections indicating the presence of a superstructure in $PbVO_3$ were detected. The highest possible non-centrosymmetric $P4mm$ space group consistent with the diffraction pattern and allowing independent shifts of atoms along the *c*-axis in a tetragonal perovskite cell was chosen for structure refinement. The program RIETAN2000 was used to achieve the best profile fitting since a strong anisotropic broadening was observed on the XPD pattern. Since the peaks of the *hk*0 zone are noticeably narrower than those of the *hkl* zone, we attributed this broadening to a strain effect. From the other side, narrow peaks of the *hk*0 zone clearly indicate the absence of an orthorhombic distortion. During the refinement the displacement parameter for the O(2) atom became slightly negative (−0.03 $Å^2$); therefore, it was fixed to 1.0 $Å^2$. This affected neither the atomic parameters nor the *R*-values. Structure information for $Pb_3(CO_3)_2(OH)_2$ and PbV_6O_{11} was taken from refs 14 and 15, respectively. Only the unit cell and profile parameters were refined for admixture phases. Experimental, calculated, and difference X-ray patterns are shown in Figure 1. Experimental data, atomic coordinates, and main interatomic distances for $PbVO_3$ are listed in Table 1.

The crystal structure of $PbVO_3$ is shown in Figure 2. It demonstrates a strong tetragonal distortion of the cubic perovskite, leading to a significant difference between the *a* and *c* parameters. As a result, the V−O(1) separation for one of the two apical oxygen atoms increases up to 2.998(5) Å, and layers of corner-shared

(8) Chamberland, B. L.; Danielson, P. S. *J. Solid State Chem.* **1974**, *10*, 249.
(9) (a) *Sovremennaya tekhnika i metody eksperimental'noi mineralogii*; Zharikov, V. A., Ivanov, I. P., Litvin, Yu. A., Eds.; Nauka: Moscow, 1985; s.280 (Russian). (b) Sirota, N. N.; Mazurenko, A. M.; Shipilo, V. B. *Izvestiya AN BelSSR, ser. Fiz.-Mat. Nauk (USSR)* **1970**, 125 (Russian).
(10) Izumi, F.; Ikeda, T. *Mater. Sci. Forum* **2000**, *321−324*, 198.
(11) Roisnel, T.; Rodriguez-Carvajal, J. *Mater. Sci. Forum* **2001**, *378−381*(1), 118.
(12) Savin, A.; Jepsen, O.; Flad, J.; Andersen, O. K.; Preuss, H.; von Schnering, H. G. *Ang. Chem. Int. End. Engl.* **1992**, *31*, 187.
(13) Krier, G.; Jepsen, O.; Burkhart, A.; Andersen, O. K. The *TB-LMTO-ASA program* Stuttgart, 1995.
(14) Martinetto, P.; Anne, M.; Dooryhee, E.; Walter, P.; Tsoucaris, G. *Acta Crystallogr. C* **2002**, *58*, 82.
(15) Mentre, O.; Abraham, F. *J. Solid State Chem.* **1996**, *125*, 91.

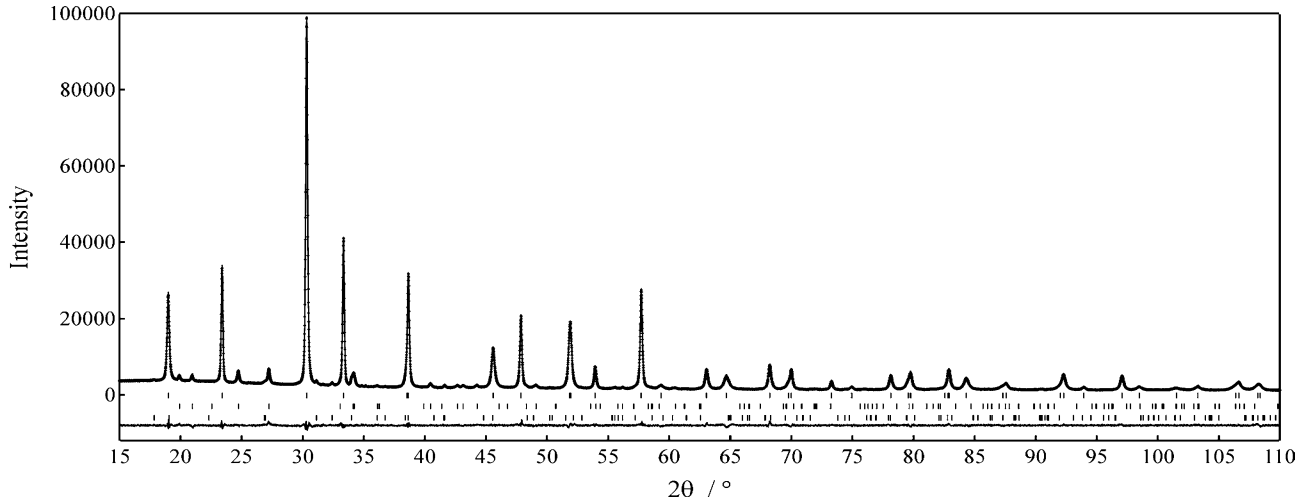

Figure 1. Experimental, calculated, and difference X-ray patterns for $PbVO_3$. Peak positions for $PbVO_3$ (up), $Pb_3(CO_3)_2(OH)_2$ (middle), and PbV_6O_{11} (bottom) are indicated.

Table 1. Experimental Data, Atomic Coordinates, Isotropic Displacement Parameters (Å²), Main Interatomic Distances (Å), and Angles (deg) for $PbVO_3$

formula	$PbVO_3$
space group	*P*4*mm* (No. 99)
temperature, K	293
a, Å	3.80005(6)
c, Å	4.6703(1)
V, Å³	67.441(2)
$\rho_{calc.}$, g/cm³	7.538
radiation, wavelength (Å)	Cu Kα_1, 1.5406
diffractometer	STADI/P
2θ range (deg)	15−110
method of refinement	Full profile
program	RIETAN2000
R_P, R_{wP}, GoF	0.026, 0.035, 1.91

phase:	$PbVO_3$	$Pb_3(CO_3)_2(OH)_2$	PbV_6O_{11}
R_I, R_F	0.015, 0.010	0.042, 0.015	0.060, 0.031
wt %	90.0	7.4	2.6

atom	*x*	*y*	*z*	B_{iso}
Pb	1/2	1/2	0.5708(3)	0.74(1)
V	0	0	0[a]	0.46(4)
O(1)	0	0	0.358(1)	1.8(1)
O(2)	1/2	0	−0.1194(9)	1.0[a]

Pb−O(1)	×4 2.388(3)	V−O(1)	×4 1.980(1)
Pb−O(2)	×4 2.865(2)	V−O(2)	×1 1.672(5)
Pb−O(1)	×4 3.742(4)	V−O(2)	×1 2.998(5)
O(1)−V−O(1)	147.3(2)	O(1)−V−O(2)	106.4(1)

[a] Fixed.

square pyramids are formed instead of a three-dimensional framework of octahedra. The vanadium atom is shifted by 0.56 Å from the square plane (formed by four O(2) equatorial oxygen atoms) toward the vertex of the pyramid, forming a short vanadyl bond. The apical V−O(1) distance is 1.672(5) Å, whereas the V−O(2) separation is 1.980(1) Å. Bond valence sum calculation[16] gives a V valence of 4.01. The Pb atom is shifted from the center of the unit cell toward one of the $[O(2)_2]$-plane. This shift is the result of the influence of the lone pair, which should be obviously located opposite to the shift direction due to steric factor. Therefore, half of the Pb−O(2) distances become noticeably shorter, 2.388(3) Å, than the other ones (3.742(4) Å), which can be considered as nonbonding. The Pb−O(1) distance is 2.865(2) Å. Thus, a tetragonal antiprism is the coordination polyhedron of the lead atom.

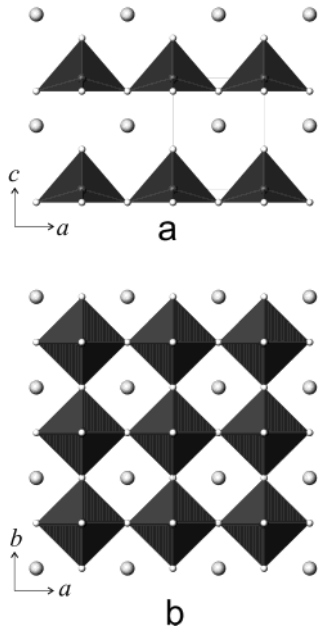

Figure 2. Two projections of the $PbVO_3$ crystal structure: (a) along the *c*-axis and (b) along the *b*-axis.

In Figure 3a we present a visualization of the ELF results, which clearly shows the presence and the localization of the lone pair of lead. As in tetragonal $PbTiO_3$ (S.G. *P*4*mm*, $a = 3.902$ Å, $c = 4.156$ Å)[17] where the short Ti−O bond (1.77 Å) is also present in TiO_6 octahedra, the shape of the lone pair is lobe-like, demonstrating the strong anisotropy of the structure.[18]

Perovskite-like oxides containing a transition metal in the B-framework often demonstrate anion nonstoichiometry, keeping the initial structural motif but with different superstructure types. This results in a change of the oxidation state of the transition metal and

(16) Schindler, M.; Hawthorne, F. C.; Baur, W. H. *Chem. Mater.* **2000,** *12,* 1248.

(17) Nelmes, R. J.; Kuhs, W. F. *Solid State Commun.* **1985**, *54*, 721.

(18) Seshadri, R. *Proc. Indian Acad. Sci. (Chem. Sci.)* **2001**, *113*, 487.

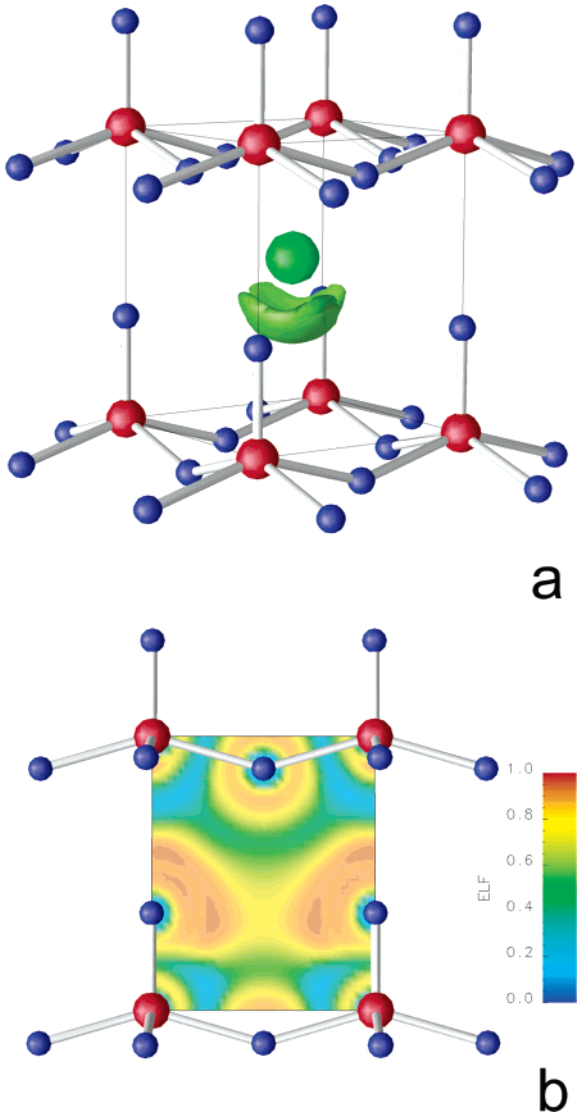

Figure 3. (a) Valence electrons ELF isosurface ($\eta = 0.85$) around Pb. (b) ELF distribution in the (100) plane.

consequently of the physical properties of the material. In the case of $PbVO_3$ we observed neither the presence of superstructure peaks in XPD patterns nor a change of the lattice parameters, which would have indicated an oxygen nonstoichiometry, even in samples prepared with starting compositions $PbVO_3 \pm \delta$ ($\delta = 0.1, 0.2, 0.3$).

Resistivity Properties and NPD Measurements. Resistivity measurements performed on a polycrystalline sample evidence semiconducting behavior, with $\rho(T)$ increasing by 3 orders of magnitude between 300 and 30 K (Figure 4). Below 30 K, the resistance becomes too high for a reliable measurement with our equipment. The increase of $\rho(T)$ is rather smooth, without clear evidence for a transition. A plot $\log(\rho)$ versus $1/T$ suggests a linear dependence and thus activated behavior in two temperature regions, one above 100 K and one between 100 and 50 K. The slopes correspond to activation energies of 340 and 180 K for $T > 100$ K and $T < 100$ K, respectively.

Unfortunately, the magnetic properties could not be determined from the susceptibility results because the susceptibility was dominated by a ferromagnetic contribution, which we attributed to be due to the PbV_6O_{11} foreign phase.[19] However, the neutron experiment allows some estimations to be made for magnetic properties of $PbVO_3$. Within the accuracy of our NPD data neither extra antiferromagnetic peaks nor an increase in the nuclear Bragg peaks were observed at the temperature $T = 1.5$ K. The estimation of the low limit of the long-range ordered ferromagnetic moment amounts to $\leq 0.05\ \mu_B$, assuming a ferromagnetic alignment of the V^{4+} spins. The estimation of the low limit of the antiferromagnetic moment is not unambiguous since the magnetic structure factors depend on a particular magnetic structure, which is not known. Assuming a simple antiferromagnetic structure in the *(ab)* plane, the low limit of the antiferromagnetic moment is $\leq 0.4\ \mu_B$.

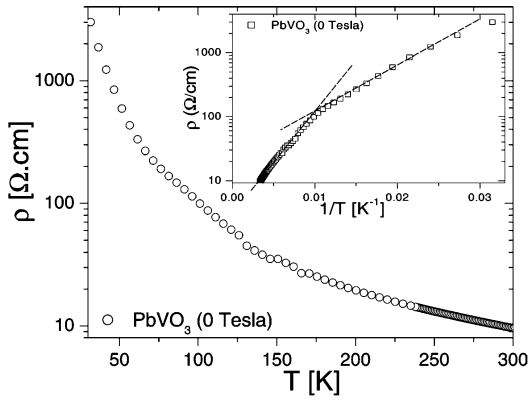

Figure 4. Temperature dependence of the resistivity of a polycrystalline $PbVO_3$ sample. Inset: Log ρ versus $1/T$ plot, showing the two regions with activated behavior (lines are guide to the eyes).

Electronic Structure from the First-Principle Study. Vanadium oxides are supposed to be systems with strongly correlated electrons;[20] for example, the true insulating and magnetically ordered states were obtained for V^{4+} oxide compounds, only taking into account the on-site Coulomb interactions.[21]

First, we performed calculations using local spin density approximation (LSDA) considering both ferromagnetic (FM) and antiferromagnetic (AFM) ordering models for $PbVO_3$. The electronic band structure was calculated using the linearized muffin-tin (MT) orbitals method within the atomic-spheres approximation.[22] We considered the unit cell with one V atom and the supercell with four V atoms to model the FM and AFM (C-type) states, respectively.

For the FM ordering, the electronic structure is found to be metallic (Figure 5a) with the near the Fermi level DOS determined by the vanadium 3d and antibonding 2p states of O(2) atom ($\mu = 0.38\ \mu$B inside the vanadium MT sphere). The character of the states near E_F evidences significant Vd−O2p hopping and suggests

(19) (a) Kato, H.; Kato, M.; Yoshimura, K.; Kosuge, K. *J. Phys.: Condens. Matter* **2001**, *13*, 9311. (b) Dhaussy, A. C.; Mentre, O.; Abraham, F.; Calage, Y. *J. Solid State Chem.* **1999**, *147*, 609.

(20) (a) Schwieger, S.; Potthoff, M.; Nolting, W. *Phys. Rev. B* **2003**, *67*, 165408. (b) Nakotte, H.; Alsmadi, A. M.; Kawanaka, H.; Kindo, K.; Goto, K. *Int. J. Mod. Phys. B* **2002**, *16*, 3058. (c) Inoue, I. H.; Bergemann, C.; Hase, I.; Julian, S. R. *Phys. Rev. Lett.* **2002**, *88*, 236403.

(21) Korotin, M. A.; Elfimov, I. S.; Anisimov, V. I.; Troyer, M.; Khomskii, D. I. *Phys. Rev. Lett.* **1999**, *83*, 1387.

(22) Weinberger, P.; Turek, I.; Szunyogh, L. *Int. J. Quantum Chem.* **1997**, *63*, 165.

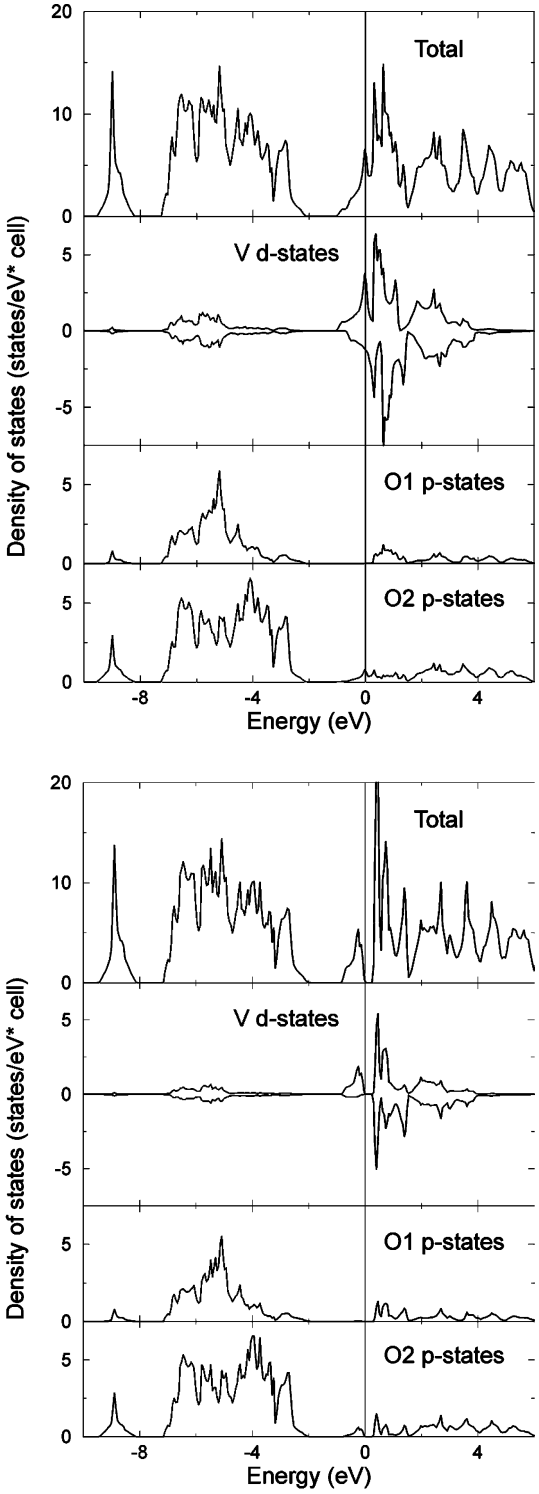

Figure 5. DOS for $PbVO_3$ calculated using a one-electron approximation: (upper panel) FM ordered structure and (bottom panel) AFM ordered structure.

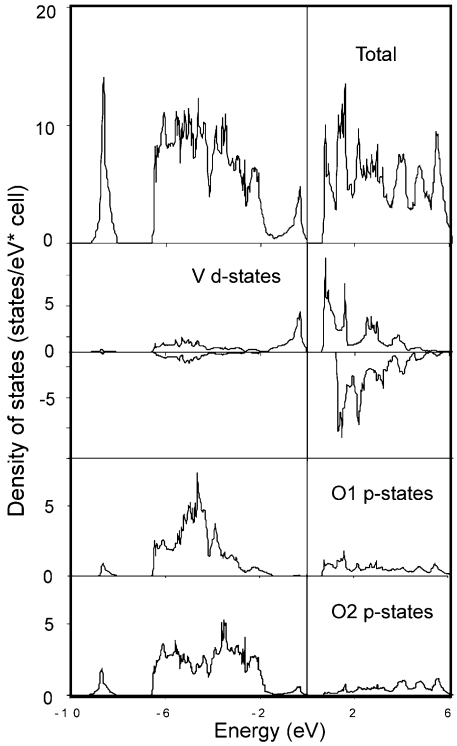

Figure 6. DOS for $PbVO_3$ calculated using LSDA+U approximation ($U = 2.0$ eV).

that the FM state is unstable. Indeed, we found that the AFM ordering in the plane has lower total energy by 66.7 meV compared to the FM one; besides, the AFM interactions result in an insulating state with indirect band gap of 0.28 eV (Figure 5b). The appearance of the band gap is due to localization of the only V^{4+} electron in the spin-up d_{xy} orbital ($\mu = 0.74\ \mu B$). It is the d_{xy} orbital that has the lowest energy in an oxygen octahedron distorted along the *z*-axis. Finally, we calculated the effective exchange interaction parameters as a second derivative of the ground-state energy with respect to the magnetic moment rotation angle. These parameters confirm the stability of the AFM magnetic configuration: we obtained strong AFM interactions in the plane ($J_{ab} \approx -29$ meV) and weak ferromagnetism along the *c* axis ($J_c = 2.9$ meV).

The NPD data observed at $T = 1.5$ K suggest the absence of long-range magnetic order. Therefore, we performed additional electronic structure calculations to take into account electron correlations by using the LSDA+U method realized in the Wien2k program package.[23] The APW+lo method was implemented and the AMF[24] scheme of the LSDA+U treatment was used. Only correlations between vanadium d electrons were accounted and only the FM case was investigated.

Introducing electron correlation potential dramatically changes the result of calculation in comparison with the one-electron approximation. Thus, $PbVO_3$ in the FM state becomes a semiconductor with E_g strongly depending on the correlation potential parameter (Figure 6): $E_g(U = 6.8\ \text{eV}) = 2.09$ eV and $E_g(U = 2.0\ \text{eV}) = 0.65$ eV. The main contribution to the DOS near the Fermi level is given by V 3d and O(2) 2p states, confirming the earlier suggestion about hopping between these electrons.

The first-principle LSDA calculations predict the insulating ground state with AFM ordering for $PbVO_3$; however, the band gap may exist also in the FM phase due to electron correlation effects. The strong dependence of the results on the approach used indicates the complexity of the real electronic structure of $PbVO_3$ and

(23) Blaha, P.; Schwarz, K.; Sorantin, P.; Trickey, S. B. *Comput. Phys. Commun.* **1990**, *59*, 399.
(24) Czyzyk, M. T.; Sawatzky, G. A. *Phys. Rev. B* **1994**, *49*, 14211.

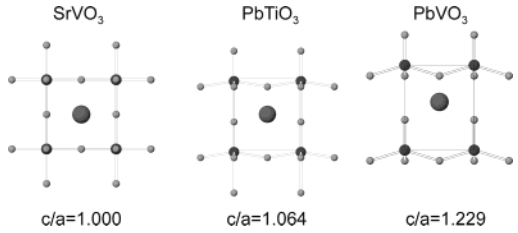

Figure 7. Tetragonal distortion of the ABO_3 perovskite.

the importance of correlations in this compound, in contrast to $SrVO_3$, which was calculated to be a simple metal.[25] No doubt that one should account for complex electron−electron interactions to obtain reliable results. However, this is a topic for a separate investigation.

Discussion

Recently, we have reported results of the synthesis and investigation of the new ternary oxide $Pb_2V_5O_{12}$ belonging to the homologous series $M_mV_{m+n}O_{3m+2n}$.[26] These structures contain so-called "plaquettes" consisting of four (for MV_nO_{2n+1}) or six (for $Pb_2V_5O_{12}$) corner-shared VO_5 square pyramids turned in the same direction. Neighboring plaquettes are edge-shared and turned in opposite directions. All "plaquette-like" structures known as MV_nO_{2n+1} series[27] and the $Pb_2V_5O_{12}$ oxide can be deduced from the parent structures with $n = \infty$ and $m = \infty$ by introducing shear planes. The $Li_xV_{2-\delta}O_{4-\delta}$ oxide[28] can be considered as a parent structure with $n = \infty$ and containing condensed VO_2 layers formed by pyramids linked by all four edges. From the other side, the AVO_3 compound with the layers of corner-shared pyramids was proposed to be another end member for this series. The latter structure obviously belongs to the perovskite family.

Perovskite-like oxides ABO_3 form a large number of structures.[29] The simplest cubic structure may undergo various kinds of distortions which in some cases result in very complicated structures. The stability of the perovskite structure can be formally estimated using the tolerance factor $t = [(r_A + r_O)]/[\sqrt{2}(r_B + r_O)] = 1$. If $t \neq 1$, the different distortion types may occur. An instability of the required ideal coordination−octahedron for B−and cubooctahedron for A-cation may be another reason for cell distortion. The Goldshmidt factors for $SrVO_3$, $PbTiO_3$, and $PbVO_3$ are 1.017, 1.027, and 1.035, respectively. $SrVO_3$ has a cubic structure, while $PbTiO_3$ has a tetragonal structure at ambient conditions[17] and becomes cubic only at high temperature.[30] $PbVO_3$ is also tetragonally distorted. In two latter structures the steric active lone pair of the Pb^{2+} cation is present, which is clearly visualized by ELF in Figure 3a. The transformation from the cubic to the tetragonal perovskite cell is shown in Figure 7.

The lone pair is the origin of the tetragonal distortion of both $PbTiO_3$ and $PbVO_3$ structures. However, there are some differences. In the $PbTiO_3$ structure the titanium atoms are shifted from the center of the octahedra, forming short and elongated Ti−O bonds (1.77 and 2.386 Å, respectively). Nevertheless, the stable octahedral coordination (c.n. = 6) of the Ti^{4+} cation keeps the three-dimensional structure motif. The important difference between TiO_6 and VO_6 [s + 4e + 1a] octahedra (where "s" implies short M−O bond, "e" equatorial, and "a" apical bonds) is that the "1a" oxygen atom opposite to the vanadyl one may be easily moved to a nonbonding distance, transforming the octahedron into a square pyramid (c.n. = 5). This is typical for V^{4+} but not for Ti^{4+}, although the vanadyl bond was not observed in other $A^{2+}VO_3$ perovskites. In comparison with $PbTiO_3$, the existence of the stable square pyramidal coordination for vanadium atoms allows in the $PbVO_3$ structure a further elongation of the *c*-parameter caused by the influence of the Pb^{2+} lone pair. One may speculate that both structural features, lone pair and vanadyl bond, acting simultaneously result in a much stronger distortion of the perovskite lattice. The $PbVO_3$ crystal structure is, apparently, an extreme case of the tetragonal distortion of the perovskite cell, connected with the transformation of VO_6 octahedra into VO_5 pyramids, which lead to a layered structure. The interaction between neighboring layers of pyramids is very weak, and that is, probably, a reason for the instability of $PbVO_3$ at ambient conditions while high pressure stabilizes this structure.

The results of the ELF calculations presented in Figure 3b allow display of the main bonding peculiarities in the $PbVO_3$ structure. The area of strong electron localization near Pb (Figure 3a) corresponds to the electron lone pair of the Pb^{2+} ion. The integration of the valence electron density over this ELF basin gives 2.14 electrons; that is quite close to the expected value for the lone pair (2 electrons). The attractor located near the vanadyl oxygen atom is the evidence for the existence of the vanadyl bond (Figure 3b). The interaction between $[VO_2]$ layers is relatively weak, which can be deduced from the presence of the strong electron delocalization area between V^{4+} and O^{2-} from neighboring layers. This conclusion is supported by calculated exchange parameters, which differ by 1 order of magnitude for in the plane and between plane interactions.

We can speculate that the transformation from an ideal octahedron in the three-dimensional $SrVO_3$ to a square pyramid with the short apical vanadyl bonding in the two-dimensional $PbVO_3$ structure is the structural reason for the change of the resistivity behavior. This decrease of dimensionality is caused by replacement of a Sr^{2+} cation by a Pb^{2+} one. A similar phenomenon was observed for the $Sr_{n+1}V_nO_{3n+1}$ compounds.[31] Thus, $SrVO_3$ is a metal and a Pauli paramagnet, while Sr_2VO_4 (K_2NiF_4-type structure) shows Curie−Weiss behavior of the magnetic susceptibility and semiconducting resistivity behavior. These differences in the properties of $SrVO_3$ and Sr_2VO_4 perovskites were at-

(25) (a) Itoh, S. *Solid State Commun*. **1993**, *88*, 525. (b) Yamazaki, M.; Tomita, N.; Nasu, K. *J. Phys. Soc. Jpn*. **2003**, *72*, 611.

(26) Shpanchenko, R. V.; Chernaya, V. V.; Abakumov, A. M.; Antipov, E. V.; Hadermann, J.; Van Tendeloo, G.; Kaul, E.; Geibel, C.; Sheptyakov, D.; Balagurov, A. M. *Z. Anorg. Allg. Chem*. **2001**, *627*, 2143.

(27) Bouloux, J. C.; Galy, J. *J. Solid State Chem*. **1976**, *16*, 385.

(28) Chirayil, T.; Zavalij, P. Y.; Whittingham, M. S. *J. Electrochem. Soc*. **1996**, *143*, L193−L195.

(29) Mitchell, R. H. *Perovskites: Modern and Ancient*; Almaz Press Inc.: Thunder Bay, Ontario, Canada, 2002; p 318.

(30) Yamaguchi, O.; Narai, A.; Komatsu, T.; Shimizu, K. *J. Am. Ceram. Soc*. **1986**, *69*, C256.

(31) (a) Giannakopoulou, V.; Odier, P.; Bassat, J. M.; Loup, J. P. *Solid State Commun*. **1995**, *93*, 579. (b) Nozaki, A.; Yoshikawa, H.; Wada, T.; Yamauchi, H.; Tanaka, S. *Phys. Rev. B* **1991**, *43*, 181.

tributed to the change in the dimensionality of the structure.

Conclusions

$PbVO_3$ is the first example of a perovskite structure containing layers of corner-shared VO_5 pyramids originating from VO_6 octahedra due to an unusually strong tetragonal distortion ($c/a = 1.23$). This compound may be considered as an extreme case of tetragonal distorted ABO_3 perovskite. Both a short vanadyl bond in the pyramids and a lone pair of Pb atoms coexist in this structure. The compound shows semiconducting behavior in $\rho(T)$. First-principle calculation indicates that correlations effects become very important, likely due to the reduction of the dimensionality from a 3D to a 2D system.

Acknowledgment. Authors are grateful to RFBR (Grant 04-03-32787) and ICDD (GiA APS91-05) for financial support. Special thanks to N. R. Khasanova, D. Sheptyakov, and S. Bushmeleva for their help in the structure refinement, N. I. Medvedeva and A. A. Gippius for their assistance in DOS calculation. This work was partially performed at the spallation neutron source SINQ, Paul Scherrer Institute, Villigen, Switzerland.

Supporting Information Available: Crystallographic information is available in CIF format. This material is available free of charge via the Internet at http://pubs.acs.org.

CM049310X